SPECIAL ISSUE

Determination of mechanisms and hydrogeological environments of Gangxianlane landslides using geoelectrical and geological data in central Taiwan

Cheng-Chao Lee · Li-Sheng Zeng · Chin-Hsien Hsieh · Chun-Yi Yu · Sheng-Hsiung Hsieh

Abstract Electrical resistivity tomography (ERT), single-point-resistance logging with time-lapse, and geological and groundwater level data, are utilized to determine the mechanism of, and a hydrogeological model of, the Gangxianlane landslide in the west-central part of Taiwan. The rock surface and geometry of the colluviums were found by integrating ERT and borehole data. The iso-resistivity line in the bedrock broadly followed the bedding plane, indicating that the contribution of lithology to resistivity exceeds that of groundwater. The results of single-point-resistance logging with time-lapse and borehole data reveal that the bedrock has low permeability, which is associated with poorly developed joints and fractures. The fine grain content part (including the clayey layer), almost parallel to the bedding plane of the bedrock and between the colluvium and the bedrock in the upper part of the landslide, served as the slip surface and is believed to have been recently produced. It can block and retain water in the colluviums. Accordingly, this slip surface has the potential to re-slip in the future. Another slope failure involved rock collapse by a well-developed open release joint close to the Huoshaoping Terrace. It is also related to groundwater flow over a large gradient from the Huoshaoping Terrace. It is a key to determining whether this landslide will expand in the future.

Keywords Landslide · Groundwater · Resistivity · Permeability · Single-point-resistance logging

C.-C. Lee (✉)
Pro Vision Environmental Engineering Corporation,
Taipei, Taiwan, ROC
e-mail: Lcc@pveec.com.tw

L.-S. Zeng
Sino Geotechnology Inc, Taipei, Taiwan, ROC

C.-H. Hsieh · S.-H. Hsieh
HCK Geophysical Company, Taipei, Taiwan, ROC

C.-Y. Yu
Department of Engineering, Ching-Yun University, Taipei,
Taiwan, ROC

Introduction

Of all geophysical characteristics, resistivity is the most sensitive to the water and clay contents. Water and clay are the main triggers of most landslides. Electrical resistivity tomography (ERT) yields continuous information about a subsurface at a much better horizontal and vertical resolution than can be achieved using conventional resistivity methods. The geometry of colluvium is always important to understanding landslides, and can be obtained easily from ERT data because of the high resistivity contrast between colluvium and the underlying basement, especially when borehole data are also considered. It is, then, the first step to determining the mechanism of a landslide. ERT is suitable for landslide surveys (McCann and Forster 1990; Lapenna et al. 2004; Perrone et al. 2004; Drahor et al. 2006; Lee et al. 2008; Marescot et al. 2008; Perrone et al. 2008; Jongmans et al. 2009). ERT is also an effective tool in hydrogeological investigations of groundwater (Šumanovac and Weisser 2001; Suzuki and Higashi 2001; Mota et al. 2004; Bauer et al. 2006; Šumanovac 2006; Frohlich et al. 2008). Additionally, it can be used to trace or monitor salinization, leakage and contamination, by the making of time-lapse measurements (Buselli and Lu 2001; Cassiani et al. 2006; Sjödahl et al. 2008; Franco et al. 2009).

The lithology and structure of stratums dominate the accumulation and transportation of groundwater.

Lithological properties include mineral composition, grain size, sorting and cementation, etc. Structure refers to the geometry of deformed rock such as its cleavages, fractures, fissures, folds, and faults. Normally, fresh rock is cemented and has low porosity. Groundwater stored in fractured joints or fissures, hence, is more complicated than unconsolidated and alluvial sediments. Groundwater data from observation wells are often adopted to obtain hydrogeological information about landslides, but they merely capture a static state of groundwater level.

The permeability of the stratum is strongly related to the distribution of groundwater; this important information must be considered in understanding landslides. In well logging, the instruments are deployed in the boreholes close to the targets; therefore, this method has the best resolution of all geophysical methods. It has been widely used in hydrogeological studies (Paillet 1993; Lile et al. 1997; Helmclark et al. 2004; Josef et al. 2009). To obtain dynamic information about groundwater and the formation of permeability, a trace test, involving single-point-resistance logging, was performed herein in this study. Generally, resistance increases with grain size but decreases as borehole diameter, density of water-bearing fractures, and concentration of borehole fluid increase. Sodium chloride (NaCl), which can markedly lower the resistance of groundwater, is inexpensive and easy to obtain; therefore, it is suitable for use as a manmade tracer for studying hydrogeological environments (Lile et al. 1997; Cassiani et al. 2006). In this study, sodium chloride was dropped into the borehole as a tracer, which could be dissolved in groundwater. The change in resistance reflects the properties of formation fluid and the conductivity of the fluid in the pores.

The assumption is made that the only variation that would be captured by time-lapse measurements is that of salinity (concentration) of groundwater, which dominates in resistance. Increasing resistance in some layers can be detected because mobile groundwater reduces the salinity of the borehole fluid. Therefore, measuring resistance not only reveals the fluids present, but also at least qualitatively indicates whether the formation is permeable. Such measurements can help to locate a fluid-filled fracture or porous material that is less resistive than solid rock.

The Gangxianlane study area is located on a hill with low elevation in central Taiwan (Fig. 1). Heavy rainfall brought by Typhoon Krosa from 5 to 7 October 2007 caused a landslide over an area of approximately 10 hectares, which interrupted traffic (Fig. 2). This study is concerned with the hydrogeological environment, the groundwater flow, and their effects on this landslide. Detailed correlations among survey results are identified to elucidate the mechanism and pattern of the landslide, which suggests means of slope protection.

Geological setting

The study area is located on the western foothills in the west-central part of Taiwan (Fig. 1). The basement is the Plio-Pleistocene Cholan Formation in the foothill, which is composed of 1,500 to 2,500 m of sandstone, siltstone, mudstone, and shale in a monotonous alternating sequence. Facies changes occur rapidly through this thick clastic sequence; no key bed that subdivides this formation into distinct members has been identified (Lee 2000). Lateritic terraces, with various elevations comprise lateritic soil and gravel unconformably, cover the Cholan Formation. They are remnants of the riverbed of the ancient Tachia River. This finding demonstrates that the high slip rate associated with uplift and mountain formation is caused by the oblique collision between the Philippine Sea plate and the Eurasian plate since late Pliocene (Fig. 1).

The topographic features, controlled by the bedding attitude, are hogback and cuesta landforms, clearly indicating that the study area and its vicinity have not major geological structure such as a fault or a fold.

The rock outcrop on steep slope faces southwest, whereas the colluviums on the gentle slop face southeast (Fig. 2). The surface of this landslide is similar to the bedding plane. Statistical analysis reveals that the bedding attitude is predominantly in the N60°E/18°S direction. Joints are also well developed on the outcrop. In particular, vertical release joints that are related to direction of the slope are easy to recognize, and most of them strike the NW–SE direction. The other joint is roughly perpendicular to the release joint, but with the same dip.

Borehole sampling

Seven continuously cored boreholes, BH-1 to BH-7 (Fig. 2), were drilled to depths of 30–80 m. Fortunately, the study area is small, and the density of boreholes is high. Based on the lithologic characteristics, the rock was divided into four layers: (1) muddy sandstone and sandstone with shale; (2) alternating muddy sandstone and shale; (3) predominantly muddy sandstone with weak-to-intense bioturbations and transported shell fragments; (4) light gray and well-sorted, middle-grained sandstone mixed with some thinly layered shale. The latter two layers, 4 ~ 6 m in thickness, can serve as key beds. Correlation between boreholes indicates that all lithological units are continuous along the bedding plane measured on the rock outcrop (Fig. 3). The BH-1 borehole on the Huoshaoping Terrace revealed that the thickness of the laterite and gravel is 8.1 m. (Fig. 4).

Unlike on the rock outcrops, a vertical release joint is rarely visible in the drilled core. The rock retained its

Fig. 1 Geological map of study area and surroundings
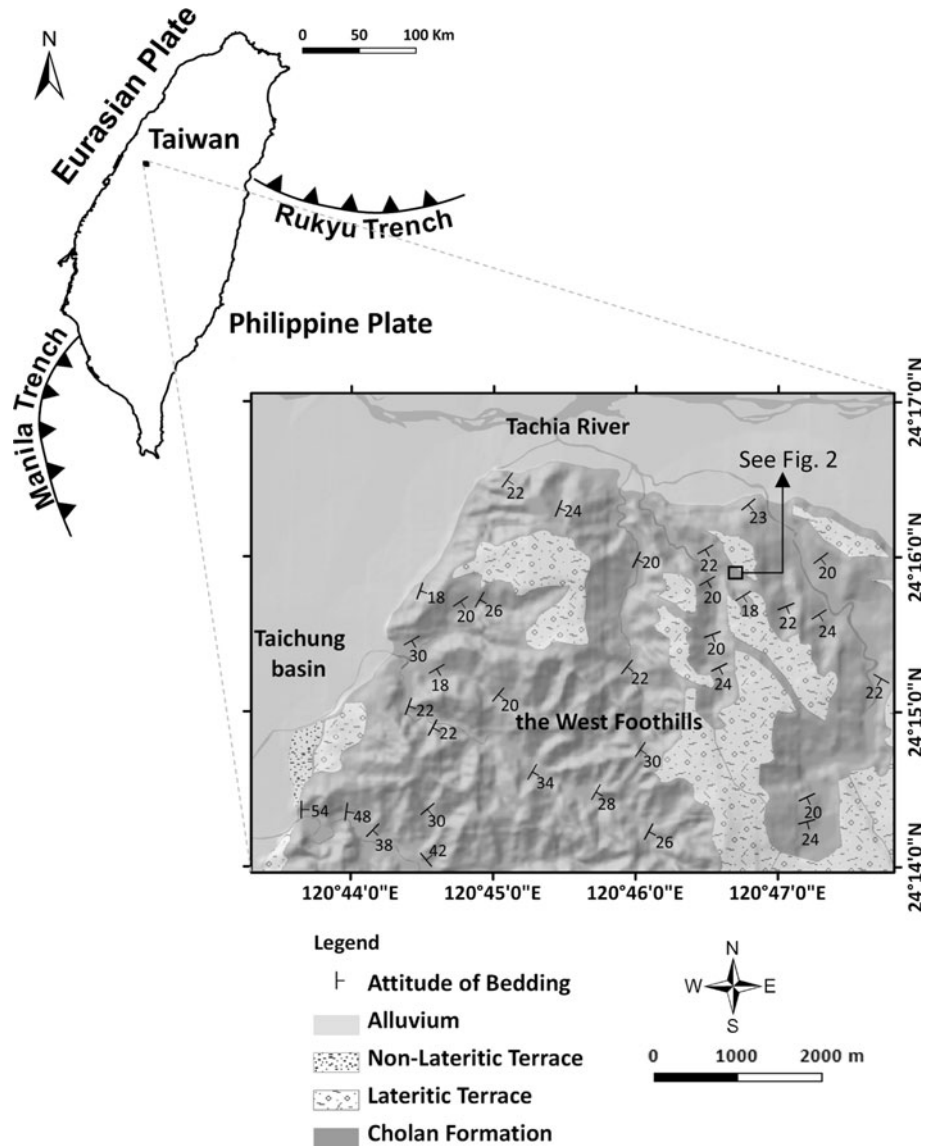
original color and was not rusted by groundwater or weathering, except for the sandstone in BH-1 above a depth of 45 m and in BH-2 at depths of 16.9–19.5 m.

The thickness of the colluvium, obtained from the borehole data except for BH-1, ranges between 1 and 7 m. Borehole data also demonstrate a viscous, clayey layer located between the colluvium and the undisturbed rock. It is centimeters thick and recently acted as a slip plane.

Geoelectrical surveys

Electrical resistivity tomography (ERT)

The ERT method is an efficient and powerful technique for mapping complex subsurface structures by measuring electrical resistivity (Griffiths and Barker 1993). High-

definition pseudosections can be quickly obtained by densely sampling apparent variations in resistivity at shallow depths. Resistivity data were acquired by using SYSCAL PRO 72 manufactured by IRIS, France with a dipole-dipole array and an electrode spacing of 5 m. This array is very sensitive to horizontal changes in resistivity and effective at mapping vertical structures (Loke 2001). The "a" electrode spacing was from 5 to 25 m, and the "n" factor, the ratio of the distance between the C1 (current electrode) and P1 (potential electrode) electrodes to the C2-C1 (or P1-P2) dipole length "a", was increased from 1 to 6 as suggested by Loke (2001). The instrument equipped with 72 channels is enough to cover the entire sections (ERT-1: 245 m, ERT-1: 205 m). To determine the true resistivity distribution of a subsurface, commercial RES2DINV software was used to perform a 2.5D smoothness-constrained inversion, using a quasi-Newton approach to reduce the

Fig. 2 Survey area map. Highest flat region is Huoshaoping Terrace. Bedding altitude is dominant in the N60°E/18°S direction
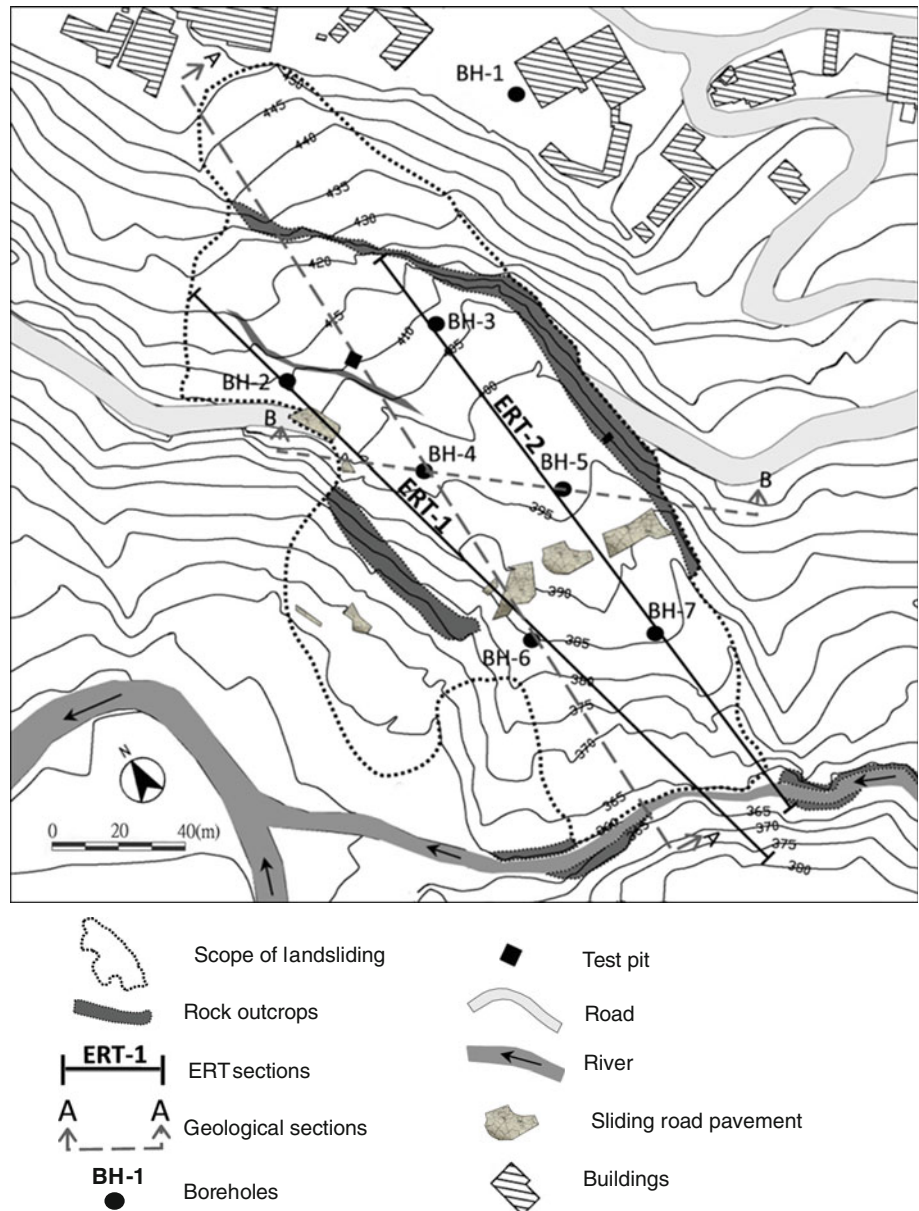
numerical calculations (Loke and Barker 1996). Each elevation of electrode was also measured for topographic correction with a moderately damped distorted grid. The final geoelectrical models show a root mean square (rms) error of 3.5–4.7% after five iterations. To smooth the variation in the iso-resistivity color bands, the final profiles were displayed using Surfer software.

Single-point-resistance logging

The electrical contact resistance between the borehole and electrical ground on the physical ground (Fig. 5) is the potential difference between the electrode on the surface and in the borehole, divided by the constant current strength, consistent with Ohm's law. The contact resistance

is a function of the resistivities and geometry of the formations between two electrodes. The ground electrode made of lead is called a mud plug, whereas the borehole electrode is considered as a probe. The resistance data were acquired by MGX Logger manufactured by Mount Sopris Instrument Co, USA, which can obtain a reading per centimeter. The velocity of probe movement is 3 m/min. After taking core, regularly spaced holes drilled on the plastic tube were set into boreholes to ensure that groundwater could freely flow immediately without a block between borehole and stratum. A fluid-filled borehole is required for resistance logging, and these logs are recorded only in the saturated part of the formation below the casing. The weight ratio of sodium chloride to water was about 1:4. The first measurement was made, prior to the injection of
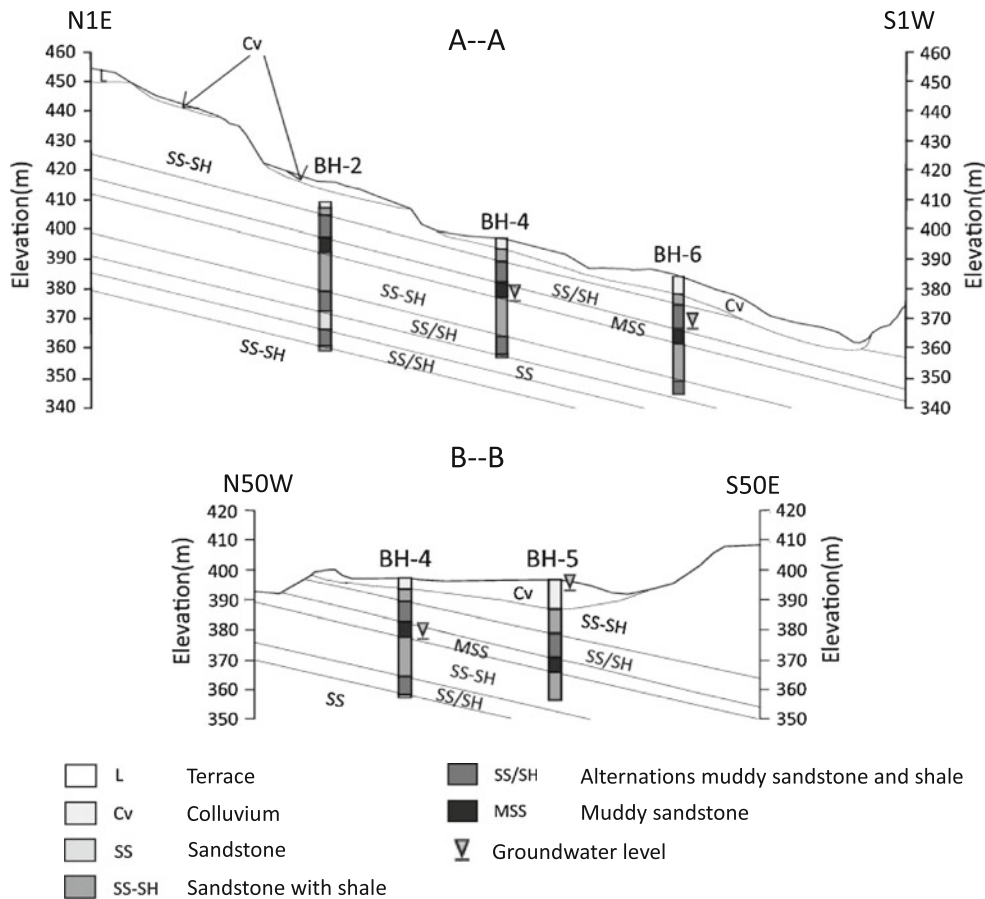
Fig. 3 Geological sections

saltwater that was injected using a water pipe into the borehole from bottom upward to above the groundwater level, whose value is regarded as the background value. The second measurement, labeled 0 min, was made after saltwater was injected. The resistance of the groundwater inside the well, read as this second measurement, is lower because the sodium chloride dissolves in the groundwater. Subsequent time-lapse measurements were made. The change in resistance depends on the salinity of the groundwater that was or was not diluted by the mobile groundwater, as determined by comparison of time-lapse measurements.

ERT results

Based on the topography after the landslide and surface geological information obtained before the core was drilled, slope failure at shallow depths was expected, and is the main target of ERT exploration. Furthermore, high dip joint as presented on the outcrops, may be detected as a discrepancy between the resistivities in areas with and without moisture.

Owing to constraints imposed by the terrain, ERT profiles were only obtained parallel to the direction of movement of the landslide, NW–SE, where the thickest colluviums should be delineated.

As revealed by the lithological character of the study area, the resistivity of the colluvium was affected by the size and amount of rock fragments, the water content, and the fine grain content. The resistivity of the rock depends on the grain size and the water content. The greater content of fines, the lower resistivity will be; water content in joints and irregular parting, will lead to the lower resistivity.

The results (Fig. 6) indicate that the resistivity variation in the colluvium is large- from greater than 100 Ωm to less than 20 Ωm. Chaotic resistivity was detected in the southern part of ERT-2 close to an unnamed river, where the mixed colluvium was interrupted with rubbish.

A high mud content in the rock, a low contrast in resistivity between fine and coarse grains and a low resolution of the thin layer all resulted in limited the variation of resistivity, from 15 to 75 Ωm. An important clue, iso-resistivity variation in the image, can be traced to identify which parameter predominantly contributes to rock
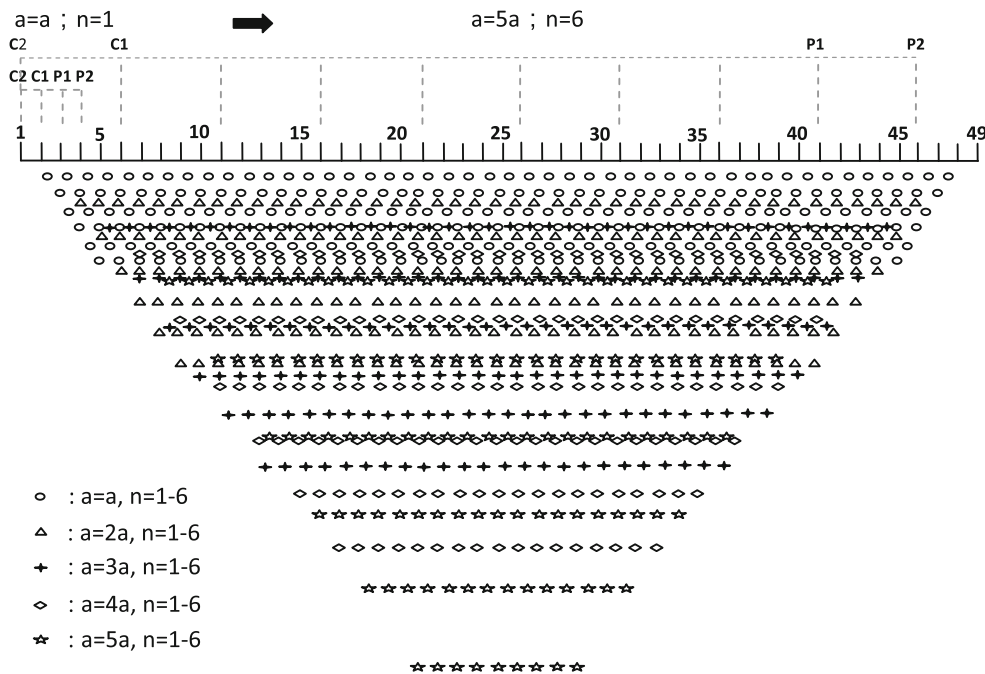
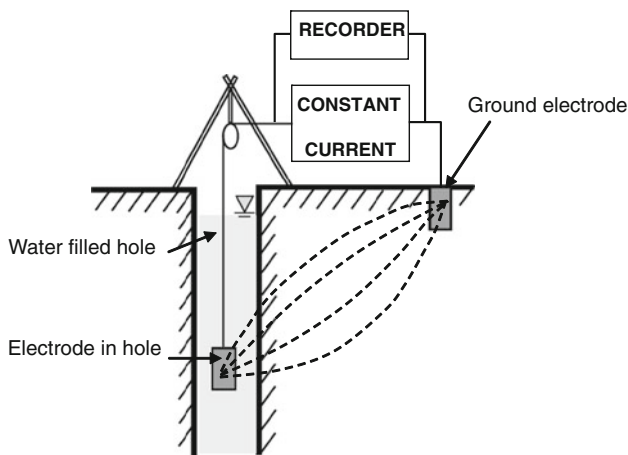Fig. 4 Pseudeosection of data points collected using dipole–dipole array

Fig. 5 Layout of single-point-resistance logging

resistivity (Lee et al. 2008). The distinct feature is that most of the iso-resistivity lines are parallel to the bedding plane of rock, indicating that the resistivity is dominated by lithology. Local and subvertical iso-resistivity lines are observed in the shallow part of rock, which may be affected by dry and subvertical joints (Fig. 6).

A low-resistivity zone in the rock between horizontal locations 30 and 50 m and below the colluviums in ERT-1 is formed by weathered brown rock and subvertical joints

therein, according to borehole BH-2 data. The groundwater level obtained from BH-2 is more than 30 m below the surface. This low-resistivity zone is considered as a path along which groundwater flows downward. It resulted in a high-resistivity zone shown in the rock between horizontal locations 53 and 63 m, where groundwater was absent.

In Fig. 6, based on borehole data, a shallow, layered low-resistivity zone (blue color tone) parallel to the slope surface is composed of moist and fine-sized grains of colluvium, a clayey layer and a large amount of shale in rock. The figure also reveals that the rock surface is close to this low-resistivity zone.

Single-point-resistance logging with time-lapse measurement

Three boreholes, BH-1, BH-5 and BH-6 (Fig. 2), were used to perform trace tests using single-point-resistance logging. The peak resistance in Ohms was found every 4 m because of overlap of the 4-m-long plastic tubes.

BH-1

The second measurement of resistance below the groundwater level of 36 m was significantly lower (0 min and red
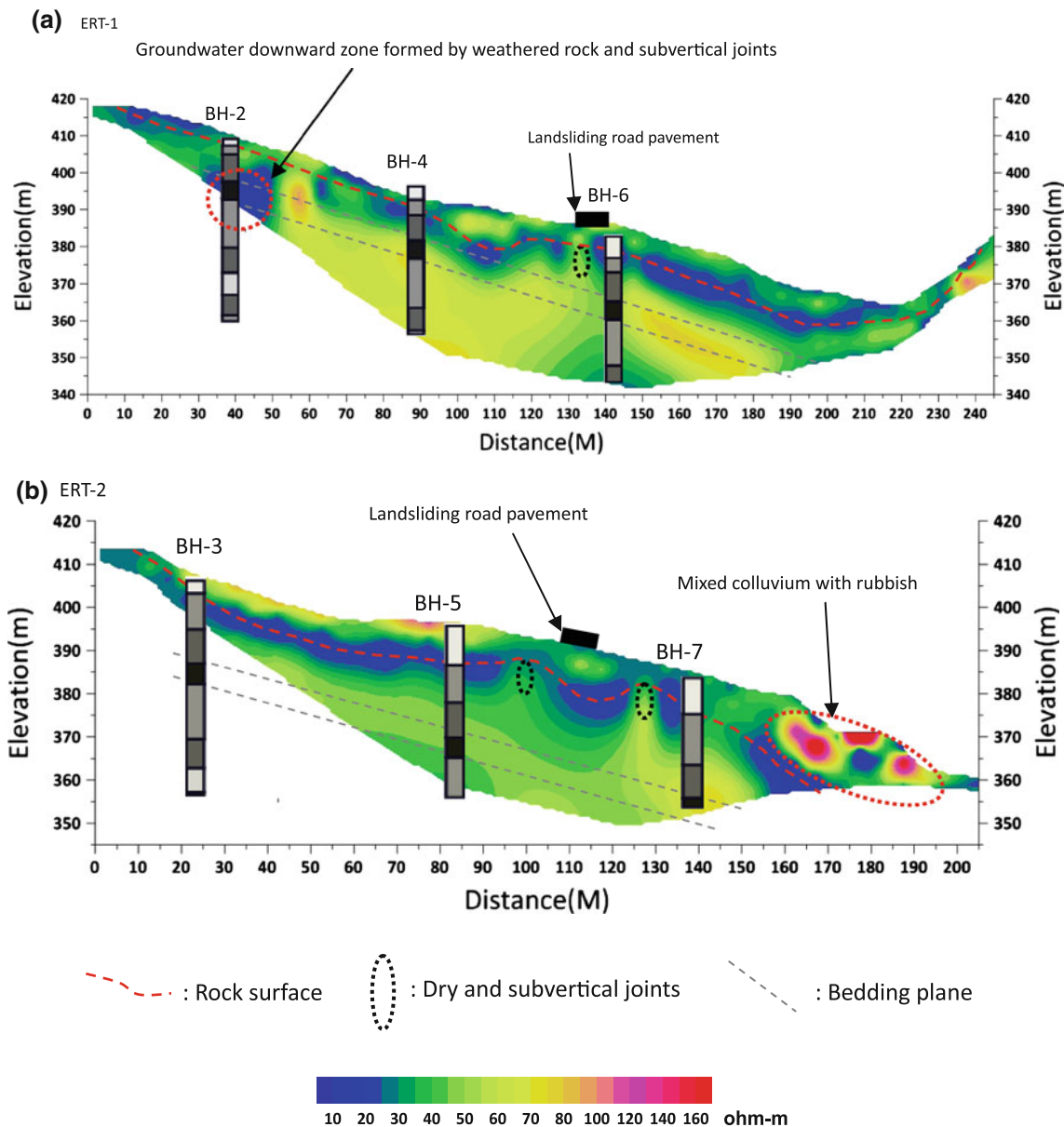
Fig. 6 Inferences from ERT and comparison with borehole data

line) than the first, because of the sodium chloride (Fig. 7a). After 40 min, the resistance was close to the background value at depths of 36–48 m (blue line), varied slightly at depths of more than 56 m, and transitioned between. The resistance at depths of more than 48 m had increased almost to the background value by 120 min, when the groundwater concentration was reduced by flow of the diluted groundwater from depths of less than 48 m.

Combining the borehole and resistance variation data yields a distinct relationship between lithology and permeability: the flow velocity of groundwater where lightly to moderately weathered sandstone dominates at depths of between 36 to 48 m, is highest; the large amount of fine

grains at depths of more than 48 m is unfavorable to groundwater flow.

BH-5

The groundwater level was approximately 2.5 m below the surface (Fig. 7b). The resistance curves at depths of more than about 7 m indicate that the resistance slowly decreases with time, because of the gravitational sinking of the sodium chloride that incompletely dissolved in groundwater. This result shows low groundwater mobility in this range because of low permeability, even in regions where the sand content is high.
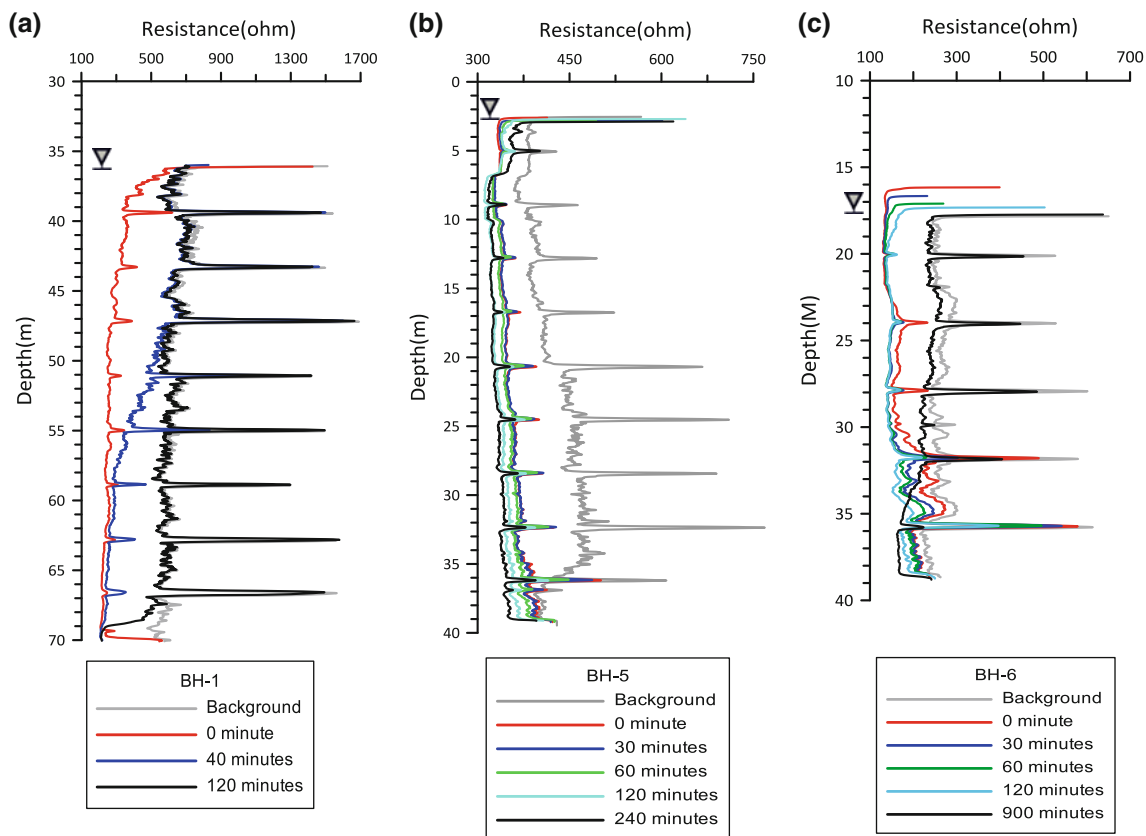
Fig. 7 Results of single-point-resistance logging with time-lapse measurement. Peaks in resistance in Ohms every 4 m correspond to overlap of 4 m-long plastic tubes. *Inverted triangles* represent groundwater level

Gradually increasing resistance was only observed at depths from 7 to 2.5 m. Furthermore, this finding implies that groundwater mobility is higher in the upper part (estimated to be 2.5 ∼ 4 m of the depth) than in the lower part.

BH-6

The groundwater level was around 17.5 m below the surface. As in BH-5, decreasing resistance from the third to fifth measurements (30, 60 and 120 min, respectively) was also found at a depth of under about 20 m, where the groundwater was almost stagnant. The resistance from 20 to 17 m gradually increased between the 60 and 120 min measurements. Just as between depths from 7 to 2.5 m in BH-5, relatively high groundwater mobility was estimated at depths of 17 to 18 m (Fig. 7c).

Moreover, the groundwater level rose from 17.5 to 16 m by the second measurement owing to an increase in the concentration of the salt solution in the well; then, it was slowly decreased to 17.5 m, the original value, over 900 min, because of the few local fissures in the rock at depths of less than 16 m.

Hydrogeological environment of landslide

The slow groundwater mobility in the rock is evident from the trace test on the landslide area. This result is supported by the fact that the dense rock that is associated with high mud content and the poor development of joints or fissures is observed in the rock samples; therefore, the permeability is low even in a thin layer with a low fine-grain content. The rock permeability near BH-6 may slightly exceed that near BH-5, because BH-6 is close to a sloped surface and is probably affected by rock release.

An unreasonable groundwater level in the colluvium was obtained at BH-5. It is much higher than that at other wells in rock (Fig. 3). Undisturbed rock, quite uniform and with low permeability, according to the results of the trace test, cannot be responsible for this abnormal fluctuation of groundwater level between wells. The accumulation of groundwater around BH-5 should be caused by the low permeability of the stratum between it and BH-7 on a downward slope. Therefore, the fine-grained part of the colluvium, associated with low permeability, acts as an aquitard and retains water from the top of the slope. This finding is supported by ERT data that demonstrate that the
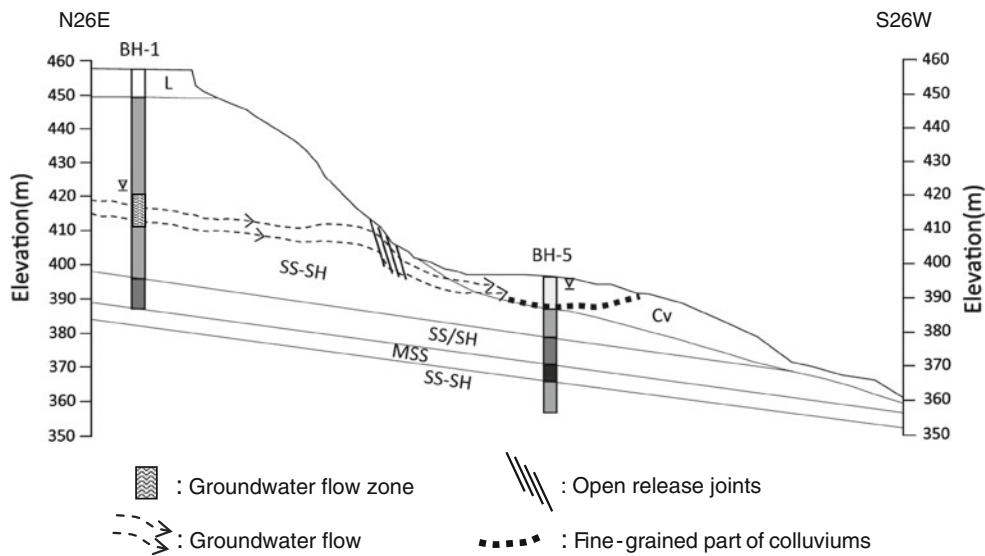
Fig. 8 Map of major groundwater flow in study area

low-resistivity zone has a curved basal surface, formed by slip in a shallow part, as displayed in Fig. 6. Furthermore, this low-resistivity zone can be reasonably inferred to extend to close to the surface between BH-4 and BH-6 in Fig. 6a, and to the surface between BH-5 and BH-7 in Fig. 6b. The large amount of water used in the trace test poured into the BH-5 and flowed out to the surface above it.

A sufficient groundwater resource is required to maintain a higher groundwater level in BH-5 than in other wells. It probably comes from the Huoshaoping Terrace to the north as determined by topographic and geological conditions (Fig. 8). The result of the trace test at BH-1 reveals that most of the area of groundwater flow is an area of weathered sandstone that is associated with better permeability, at depths of between 36 and 48 m. The difference between the groundwater heads of BH-1 and BH-5, around 30 m, provides a large hydraulic gradient for groundwater. This is a major cause of the high groundwater velocity between depths of 36 and 48 m as estimated from the rapid increase in resistance in an interval of 40 min.

The salient feature on the steep rock slope with a NW strike direction, north of BH-3 and below the Huoshaoping Terrace (Fig. 2), is the development of subvertical joints, especially open release joints, where cut rock with a pillar-form can easily collapse directly or slip along the bedding plane. Either process results in retrogression of the slope around the Huoshaoping Terrace.

The groundwater from the Huoshaoping Terrace infiltrates into the release joints close to the rock surface of the steep slope, increasing the groundwater pressure in them and the tension force in the surrounding rock (Fig. 8). This phenomenon may explain why the other steep rock slopes

in the area of this landslide exhibit fewer failures that are associated with joints due to low groundwater. In addition to groundwater, the surface water that remains after intense precipitation is critical to failure of the surface slope in the rainy season.

Mechanism of landslide

The surface of the slope, in the N70°E/20°S direction that was covered by colluviums above the sliding road, is similar to the bedding plane of rock. Its bedrock is prone to planar failure. The toe of the slope is cut by an unnamed river with an N15°E strike whose northern side is gentle colluviums and southern side is a steep rock slope, resembling the original before the landslide. Topography suggests that planar failure is likely to be caused by erosion of the river at its toe. Strictly, however, the slope in the N75°W/22°S direction between the sliding road pavement and the unnamed river is not a dip slope. Therefore, the underlying and deep rock was not involved in the last landslide. The ERT data also indicate that the thickness of the colluvium near the toe of the slope increased, implying that it was formed at an earlier time before the last landslide. This phenomenon may be related to the erosion of the toe of the slope by the river.

According to an interview with local residents, before the landslide, surface water frequently accumulated on the original road and its upward slope during intense rainfall, reflecting the fact that an excess of surface water cannot be drained away by a poor surface drainage system. However, the water in the colluviums did not tend to infiltrate the rock. The position of the zone of relatively low

permeability in the colluviums or the between colluviums and the rock is very similar to the situation after the landslide, as mentioned above. Consequently, the amount of water in the colluviums rapidly increased over a short time, reducing the effective stress of the slope and increasing the downward force of the slope. The extremely shallow rock may have been involved in any slippage. Based on the ERT (Fig. 6), the low-resistivity zone with a somewhat curved basal surface in shallow, upper part of the slope, demonstrates this feature. This is first step in the slope failure, directly pushing down the slope southeastward and southwestward, where the poorly cohesive colluviums were caused to further collapse, but not reaching the deep rock. ERT data from the lower part of the slope also do not reveal low resistivity that was caused by slip between colluviums and rock as in the upper part.

Clearly, the development of a landslide is strongly affected by the low-permeability zone in the shallower part of slope, including the thin clayey layer or the area of high fine grain content. The thin clayey layer is formed by slip; the latter is formed by the weathering of colluviums.

A 2 × 2 × 2.5 m test pit (Fig. 2) was excavated to observe directly and closely the contact between colluvium and rock. The profile, obtained by excavation using a power shovel, shows from top to bottom, colluvium, a clayey layer and rock. The profile exhibited good horizontal continuity, even though the clayey layer varied in thickness from 2 to 10 cm only. It is believed to have formed in the last landslide (on 5 to 7 October, 2007). The colluvium easily collapsed during the excavation, because it contained a large amount of water, whereas the massive rock was almost dry. Therefore, the clayey layer has low permeability, and can block surface water from passing through the colluvium into the rock.

In contrast, the rock part of slope is stable, and the level of most of the groundwater in the rock, determined from the wells, is more than 10 m below the rock surface, except at BH-5. Increased by 2 to 6 m under intense precipitation, based on more than one year of monitoring data; but this effect still did not negatively affect the stability of the whole slope. The long-term data obtained using inclinometers also indicate that the displacement of the rock is less than 12 mm and was in no particular direction. No potential weak zone formed by slippage is present in the rock.

Two forms of failure of the slope can still occur in the future: one may occur in colluviums with a large amount of water; the clayey layer associated with the low permeability is a potential re-slip surface. The erosion of the toe of the slope by rising river water is another potential cause of the collapse of the thicker colluvium down the slope. The other type of failure is rock collapse by well-developed release joints on the steep slope, especially near the

Huoshaoping Terrace where such potential collapse is a key to determining whether the area of failure slope may be expanded.

Conclusion

The groundwater system in the region of a landslide, at least above the sliding road, is divided by the fine grain content (including the clayey layer) with low permeability as an aquitard between colluviums and rock. The colluvium and rock have their own groundwater levels as expected, even though only a groundwater level in the rock was obtained from the wells.

Based on geophysical and geological data, the following conclusions are drawn.

1. The iso-resistivity lines in the bedrock in the landslide area that is covered by colluviums are similar to those in the bedding plane, suggesting that the contribution of lithological character to the resistivity is higher than that of groundwater. Low permeability and poorly developed joints and fractures are thus inferred. This result was confirmed by the single-point-resistance logging and data from boreholes.
2. The release joint, which may or may not be open, is strongly related to groundwater level; and its flow close to the Huoshaoping Terrace, the open release joint is well developed. The rock, cut by joints, can easily collapse. This situation is associated with the groundwater flow over a high gradient from the Huoshaoping Terrace. This rock slope must be protected from groundwater and is a key to determining whether the area of failure slope will be expanded.
3. Owing to low permeability of thin clayey layer between the colluvium and the rock, when a large amount of water accumulates in the colluvium, the resistance of this layer is reduced and the downward force of the slope is increased; therefore, this layer is a potential re-slip surface. Furthermore, high fine grains' content in the colluvium results in low permeability, which has a similar effect. Hence, the colluviums importantly contribute to landslides, in which extremely shallow rock may be involved.
4. The erosion of the toe of the slope by the river is also a trigger of the collapse of the thicker colluvium. A revetment should be established on the toe of the slope to prevent erosion and deterioration by the unnamed river, and a surface drainage system is required.

References

Bauer P, Supper R, Zimmermann S, Kinzelbach W (2006) Geoelectrical imaging of groundwater salinization in the Okavango Delta. Botswana Journal of Applied Geophysics 60:126–141

Buselli G, Lu K (2001) Groundwater contamination monitoring with multichannel electrical and electromagnetic methods. Journal of Applied Geophysics 48:11–23

Cassiani G, Bruno V, Villa A, Fusi N, Binley AM (2006) A saline trace test monitored via time-lapse surface electrical resistivity tomography. Journal of Applied Geophysics 59:244–259

Drahor MG, Göktürkler G, Berge MA, Özgür Kurtulmuş T (2006) Application of electrical resistivity tomography technique for investigation of landslides: a case from Turkey. Env Geol 50:147–155

Franco R, Biella G, Tosi L, Teatini P, Lozej A, Chiozzotto B, Giada M, Rizzetto F, Claude C, Mayer A, Bassan V, Gasparetto-Stori G (2009) Monitoring the saltwater intrusion by time lapse electrical resistivity tomography: The Chioggia test site (Venice Lagoon, Italy). Journal of Applied Geophysics 69:117–130

Frohlich RK, Barosh PJ, Boving T (2008) Investigating changes of electrical characteristics of the saturated zone affected by hazardous organic waste. Journal of Applied Geophysics 64:25–36

Griffiths DH, Barker RD (1993) Two-dimensional resistivity imaging and modelling in areas of complex geology. Journal of Applied Geophysics 29:211–226

Helmclark CM, Rodgers DW, Smith RP (2004) Borehole geophysical techniques to define stratigraphy, alteration and aquifers in basalt. Journal of Applied Geophysics 55:3–38

Jongmans D, Bièvre G, Renalier F, Schwartz S, Beaurez N, Orengo Y (2009) Geophysical investigation of a large landslide in glaci-olacustrine clays in the Trièves area (French Alps). Eng Geol 109:45–56

Josef VD, Miroslav K, Martin P (2009) Well logging methods in groundwater surveys of complicated aquifer systems: Bohemian Cretaceous Basin. Env Geol 57:1021–1034

Lapenna V, Lorenzo P, Perrone A, Piscitelli S, Rizzo E, Sdao F (2004) 2D electrical resistivity imaging of some complex landslides in the Lucanian Apennine chain, southern Italy. Geophysics 70:B11–B18

Lee JF (2000) Explanatory text of the geological map of Taiwan, sheet 18: Tungshih. Centr Geol Surv, Taipei, Taiwan

Lee CC, Yang CH, Liu HC, Wen KL, Wang ZB, Chen YJ (2008) A Study of the hydrogeological environment of the lishan landslide area using resistivity image profiling and borehole data. Eng Geol 98:115–125

Lile OB, Morris M, Rønning JS (1997) Estimating groundwater flow velocity from changes in contact resistance during a saltwater tracer experiment. Journal of Applied Geophysics 38:105–114

Loke MH (2001) Tutorial: 2-D and 3-D electrical imaging surveys. http://www.geoelectrical.com

Loke MH, Barker RD (1996) Rapid least-squares inversion of apparent resistivity pseudosections by a quasi-Newton method. Geophys Prospect 44:499–524

Marescot L, Monnet R, Chapellier D (2008) Resistivity and induced polarization surveys for slope instability studies in the Swiss Alps. Eng Geol 98:18–28

McCann DM, Forster A (1990) Reconnaissance geophysical methods in landslide investigations. Eng Geol 29:59–78

Mota R, Monteiro Santos FA, Mateus A, Marques FO, Goncalves MA, Figueiras J, Amaral H (2004) Granite fracturing and incipient pollution beneath a recent landfill facility as detected by geoelectrical surveys. Journal of Applied Geophysics 57:11–22

Paillet FL (1993) Using borehole geophysics and cross-borehole flow testing to define hydraulic connections between fracture zones in bedrock. Journal of Applied Geophysics 30:261–279

Perrone A, Iannuzzi A, Lapenna V, Lorenzo P, Piscitelli S, Rizzo E, Sdao F (2004) High-resolution electrical imaging of the Varco d', Izzo earthflow (sourthern Italy). Journal of Applied Geophysics 56:17–29

Perrone A, Vassallo R, Lapenna V, Di Maio C (2008) Pore water pressures and slope stability: a joint geophysical and geotechnical analysis. Journal of Geophysics Engineering 5:323–337

Sjödahl P, Dahlin T, Johansson S, Loke MH (2008) Resistivity monitoring for leakage and internal erosion detection at Hällby embankment dam. Journal of Applied Geophysics 65:155–164

Šumanovac F (2006) Mapping of thin sandy aquifers by using high resolution reflection seismics and 2-D electrical tomography. Journal of Applied Geophysics 58:144–157

Šumanovac F, Weisser M (2001) Evaluation of resistivity and seismic methods for hydrogeological mapping in karst terrains. Journal of Applied Geophysics 47:13–28

Suzuki K, Higashi S (2001) Groundwater flow after heavy rain in landslide-slope area from 2-D inversion of resistivity monitoring data. Geophysics 66:733–743